Disruption of snRNP biogenesis factors Tgs1 and pICln induces phenotypes that mirror aspects of SMN-Gemins complex perturbation in *Drosophila*, providing new insights into spinal muscular atrophy

Rebecca M. Borg [a,b,c], Benji Fenech Salerno [a,b], Neville Vassallo [a,b], Rémy Bordonne [c], Ruben J. Cauchi [a,b,*]

[a] Department of Physiology and Biochemistry, Faculty of Medicine and Surgery, University of Malta, Msida, Malta
[b] Centre for Molecular Medicine and Biobanking, Biomedical Sciences Building, University of Malta, Msida, Malta
[c] Institut de Génétique Moléculaire de Montpellier, CNRS-UMR5535, Université Montpellier 1 and 2, Montpellier, France

ARTICLE INFO

ABSTRACT

The neuromuscular disorder, spinal muscular atrophy (SMA), results from insufficient levels of the survival motor neuron (SMN) protein. Together with Gemins 2–8 and Unrip, SMN forms the large macromolecular SMN-Gemins complex, which is known to be indispensable for chaperoning the assembly of spliceosomal small nuclear ribonucleoproteins (snRNPs). It remains unclear whether disruption of this function is responsible for the selective neuromuscular degeneration in SMA. In the present study, we first show that loss of wmd, the *Drosophila* Unrip orthologue, has a negative impact on the motor system. However, due to lack of a functional relationship between wmd/Unrip and Gemin3, it is likely that Unrip joined the SMN-Gemins complex only recently in evolution. Second, we uncover that disruption of either Tgs1 or pICln, two cardinal players in snRNP biogenesis, results in viability and motor phenotypes that closely resemble those previously uncovered on loss of the constituent members of the SMN-Gemins complex. Interestingly, overexpression of both factors leads to motor dysfunction in *Drosophila*, a situation analogous to that of Gemin2. Toxicity is conserved in the yeast *S. pombe* where pICln overexpression induces a surplus of Sm proteins in the cytoplasm, indicating that a block in snRNP biogenesis is partly responsible for this phenotype. Importantly, we show a strong functional relationship and a physical interaction between Gemin3 and either Tgs1 or pICln. We propose that snRNP biogenesis is the pathway connecting the SMN-Gemins complex to a functional neuromuscular system, and its disturbance most likely leads to the motor dysfunction that is typical in SMA.

© 2016 Elsevier Inc. All rights reserved.

1. Introduction

The neuromuscular disorder, spinal muscular atrophy (SMA), is the leading genetic cause of infant death. Hallmark features include loss of spinal motor neurons as well as atrophy of the proximal limb and intercostal muscles. Available therapies are, at best, palliative. In the majority of cases, SMA is the result of insufficient levels of the ubiquitously-expressed survival motor neuron (SMN) protein (Burghes and Beattie, 2009; Monani and De Vivo, 2014). Together with Gemins 2–8 and Unrip, SMN forms the large macromolecular SMN-Gemins complex that is indispensable for chaperoning a key step in the biogenesis of small nuclear ribonucleoproteins (snRNPs), the core constituents of the spliceosome (Cauchi, 2010). It has recently been proposed that this function forms part of a broader role by the SMN-Gemins complex

in RNP exchange (So et al., 2016). Whether SMA results from a disruption in snRNP biogenesis and the consequential pre-mRNA missplicing of an ensemble of genes that are critical for the function of the neuromuscular system is still unclear (Burghes and Beattie, 2009; Li et al., 2014; Workman et al., 2012). Predominantly supported by the localisation of its constituent members in transport granules within neuronal processes, the SMN-Gemins complex has been implicated in the axonal trafficking of mRNAs and an alternative hypothesis proposing that disruption of this non-canonical function is responsible for SMA's signature features has gained traction in recent years (Burghes and Beattie, 2009; Fallini et al., 2012).

The production cycle of Sm-class snRNPs involves a cytoplasmic phase in which the SMN-Gemins complex collaborates with the protein arginine methyltransferase 5 (PRMT5) complex to regulate the coupling of a heptameric ring of Sm proteins with small nuclear RNAs (snRNAs) thereby generating the snRNP core structure. Key events in this process were unravelled through extensive biochemical and structural studies *in vitro*. In the early assembly phase, nascent Sm proteins are sequestered by the PRMT5 complex, which unites WD45/MEP50, PRMT5 and

pICln. A bound Sm protein subset (B/B′, D1 and D3) is symmetrically dimethylated on designated arginine residues by PRMT5 and, possibly PRMT7, a modification thought to enhance their affinity for the SMN-Gemins complex (Fischer et al., 2011). The conclusion of this phase is marked by the formation of two distinct Sm protein sub-complexes each sharing pICln, which prevents premature RNA interactions (Chari et al., 2008; Grimm et al., 2013).

Acceptance by the SMN-Gemins complex of the pre-organised Sm proteins from the pICln-D1/D2/F/E/G and pICln-B/D3 intermediates in parallel with the simultaneous dismissal of pICln propels the reaction into the late assembly phase (Chari et al., 2008; Grimm et al., 2013). Gemin2 handles the majority of Sm proteins by wrapping itself around the crescent-shaped Sm D1/D2/F/E/G pentamer and blocking RNA binding capacity until delivery of nuclear-exported snRNAs by Gemin5 (Battle et al., 2006; Grimm et al., 2013; Lau et al., 2009; Yong et al., 2010; Zhang et al., 2011). Unrip is required for Sm ring closure, during which the Sm B/D3 dimer replaces the Gemin6/Gemin7 dimer, a structurally-similar temporary surrogate around which the Sm pentamer might be initially arranged (Ma et al., 2005; Ogawa et al., 2009). The remodelling of RNA, and, eventually, RNP molecules during the assembly reaction is most probably fulfilled by DEAD-box RNA helicase Gemin3 (Charroux et al., 1999; Yan et al., 2003), although precise information in this regard is lacking. Prior to nuclear import, the 7-methylguanosine (m^7G) cap of assembled snRNPs is hypermethylated to a 2,2,7-trimethylguanosine (TMG) cap (Mouaikel et al., 2002), which along with the Sm ring acts as a nuclear-localisation signal (Fischer et al., 2011). The key player in this process is trimethylguanosine synthase 1 (Tgs1), which is thought to be recruited by the SMN-Gemins complex (Mouaikel et al., 2003).

The fruit fly *Drosophila melanogaster* is an attractive model system to study the *in vivo* function of human orthologues (Bellen and Yamamoto, 2015). To this end, we have previously shown that SMN and its Gemin associates participate in a common pathway that is essential for the correct function of the motor system (Borg and Cauchi, 2013; Borg et al., 2015). In contrast to the elaborate nine-membered human version, *Drosophila* is thought to possess a simpler SMN-Gemins complex that includes SMN, Gemin2, Gemin3 and Gemin5 as its constituent members (Cauchi et al., 2010). Bioinformatic analyses exclude the presence of additional orthologues with the exception of Unrip (also known as serine-threonine kinase receptor-associated protein or Strap) (Cauchi, 2010). In the present study, we first sought to investigate whether wmd, the *Drosophila* Unrip orthologue, has similar tissue-specific requirements as those reported for other members of the SMN-Gemins complex. Interestingly, we find that loss of wmd/Unrip function in the motor unit gives rise to viability and/or motor defects. However, we could detect neither a functional relationship nor a direct association between wmd/Unrip and Gemin3, hence, raising the possibility that wmd/Unrip works outside of the SMN-Gemins complex in *Drosophila* and was only added to the complex later in evolution.

We next asked whether the involvement of the SMN-Gemins complex in snRNP biogenesis is imperative for a functional neuromuscular system *in vivo*. To this end, we examined phenotypes resulting from the disruption of Tgs1 or pICln, two cardinal players in the snRNP biogenesis pathway, which have never been directly linked to axonal RNA metabolism. Intriguingly, we uncover that similar to SMN-Gemins complex members, both snRNP biogenesis factors are required for normal motor behaviour. Furthermore, overexpression of either Tgs1 or pICln in a pan-muscular pattern in wild-type flies has deleterious effects on adult viability and neuromuscular activity, a situation analogous to that reported for Gemin2 (Borg et al., 2015). Toxicity is conserved in the yeast *Schizosaccharomyces pombe* (*S. pombe*), in which we find that the cytoplasmic retention of Sm proteins, likely indicating a block in snRNP biogenesis, is a contributing factor. Importantly, we show a strong genetic interaction and a physical association between Tgs1 or pICln and Gemin3. Our results provide convincing evidence favouring snRNP biogenesis as the pathway connecting the SMN-Gemins complex to optimal neuromuscular performance.

2. Results

2.1. wmd, the Drosophila orthologue of Unrip, is an essential gene

The *Drosophila* orthologue of WD-repeat protein Unrip has a high degree of homology to its vertebrate counterparts including human (55% identity; 80% similarity) throughout the entire length of the protein (Supplementary information, Fig. S1). Based on the improper lamination of dorsal and ventral wing surfaces observed in homozygotes with a *P*-element insertional mutation, Dworkin and Gibson (2006) named the gene *wing morphogenesis defect* or wmd. Knockdown of wmd/Unrip through the expression of an RNAi transgene (*wmd-IR^STARK*) targeting the 5′ untranslated region (UTR) shows that a ubiquitous reduction of wmd function leads to lethality. This outcome is obvious either when the high-expressing *α-Tub*-GAL4 driver is used or, in case of the low-expressing *da*-GAL4 driver, at culture temperatures that permit maximal GAL4 activity (29 °C) (Fig. 1A). As evidence of the specificity of the RNAi-based knockdown, we first demonstrate that escapers, in which RNAi is driven by *da*-GAL4 at lower culture temperatures (25 °C), have wing defects that are similar to those of flies that are transheterozygous for *wmd^Matt*, a 5′ UTR *P*-element insert (Supplementary information, Fig. S2), and a chromosomal deficiency (*Df[2R]BSC661*) that covers wmd amongst other genes (Fig. 1B–D). Secondly, expression of wmd mRNA was dramatically reduced in larvae with an RNAi-induced knockdown in all tissues (*da*-GAL4 > *wmd-IR-STARK*) compared to controls (*da*-GAL4/+). No effect on the expression level of the housekeeping control *tat-binding protein-1* (*tbp-1*) was observed in larvae of either genotype (Fig. 1E).

2.2. wmd/Unrip is required for normal motor behaviour

We next asked whether wmd is required in the motor system. We found this to be the case. Hence, the lethality or reduced adult viability attributed to ubiquitous wmd knockdown can be recapitulated when knockdown is restricted to muscle tissues via the strong pan-muscular *how*-GAL4 and *C179*-GAL4 drivers at maximal GAL4 activity (29 °C). The phenotype is, however, more pronounced when RNAi driven by the pan-muscular *Mef2*-GAL4 driver, is enhanced by extra levels of Dicer-2 (Fig. 1A). Turning to the central nervous system (CNS), we show that pan-neuronal wmd reduction via the *elav*-GAL4 driver in combination with increased Dicer-2 levels results in lethality when flies are cultured at 29 °C. Since at lower temperatures flies with the same genotype (*elav*-GAL4 > *Dcr-2* + *wmd-IR^STARK*) are adult viable, they were analysed for defects in motor function via a flight assay in which the height a fly falls in a cylinder determines its flight performance. Intriguingly, we show that flies exhibit an age-dependent progressive decline in flight performance. In this regard, starting at day 5 post-eclosion, a significant number of organisms are non-fliers, which do not stick to the walls of upper sectors, hence, dropping to lower sectors (Fig. 2A). Survival of the organisms throughout adulthood was also significantly affected (Fig. 2B). We have recently reported that muscle-restricted changes in the levels of SMN, Gemin2 or Gemin5 precipitate motor and viability defects associated with the Gemin3 hypomorph *Gem3^BART* (Borg et al., 2015). In this context, enquiring whether the same is also true for wmd, we found that in combination with Gem3-^BART, wmd knockdown in muscle had no effect on flight ability (Fig. 2A) or lifespan (data not shown) throughout adulthood. Despite the lack of a genetic interaction between wmd/Unrip and Gemin3, overall, these findings reveal a key requirement for wmd/Unrip in the motor system.

2.3. Depletion of Tgs1 in either muscle or neurons has a deleterious effect on adult viability

Tgs1 is a highly conserved enzyme that shows the highest homology at its C-terminus, the site of the methytransferase domain
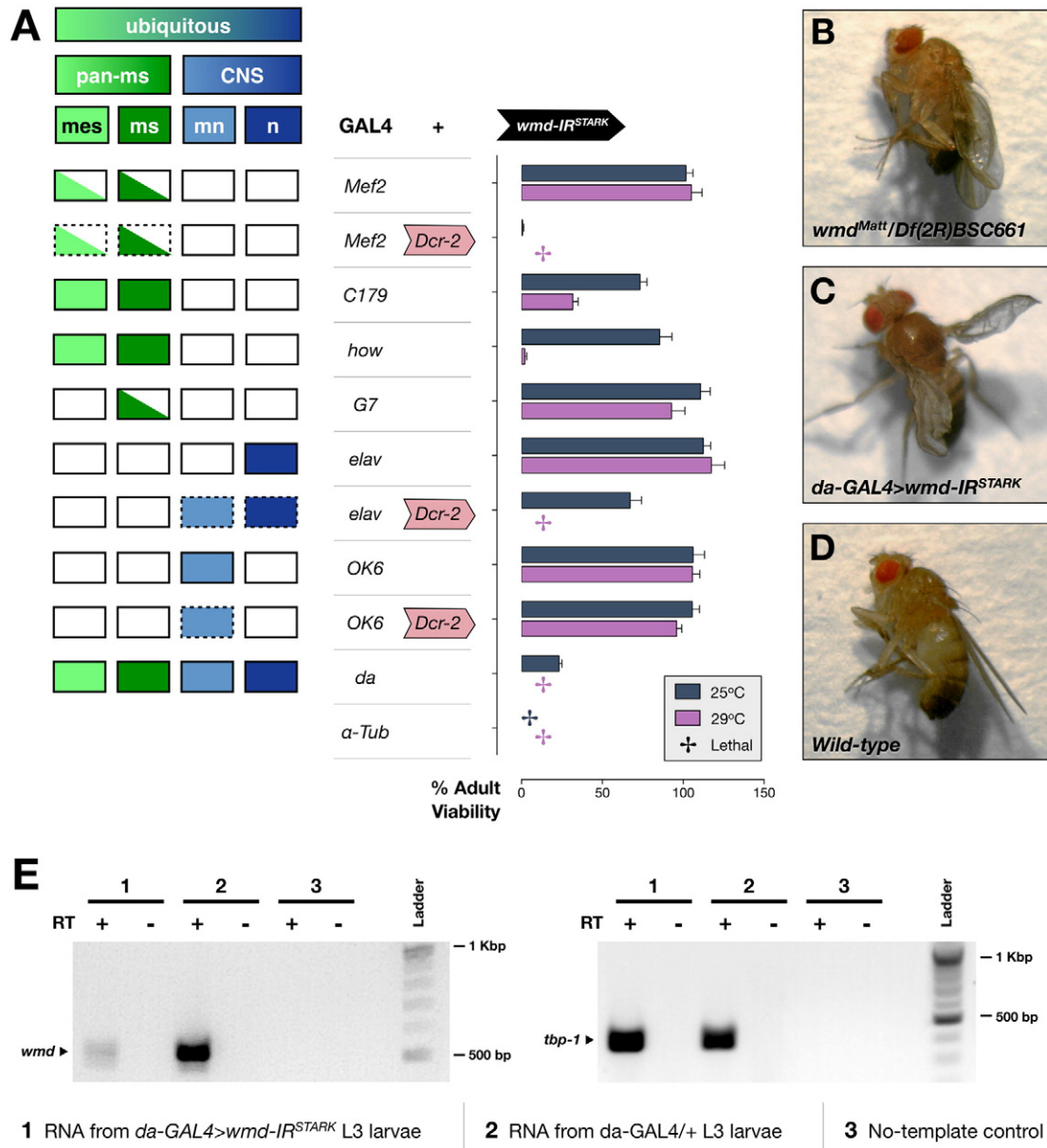
Fig. 1. Adequate levels of wmd/Unrip in muscle and neurons are required for viability. (**A**) RNAi-mediated knockdown of wmd leads to lethality or reduced viability when expression of an RNAi transgene targeting wmd mRNA transcripts (wmd-IR^{STARK}) is driven in a ubiquitous pattern via the α-Tub-GAL4 and da-GAL4 drivers. This outcome can be replicated if wmd depletion is restricted to either muscle (Mef2-GAL4, C179-GAL4 and how-GAL4) or neurons (elav-GAL4). Effects are most obvious at temperatures associated with maximal GAL4 activity (29 °C) and/or in the presence of enhanced Dicer-2 (Dcr-2) levels, two strategies employed to heighten the knockdown effect. *Left panel*: Tissue expression pattern of GAL4 drivers. *Right panel*: bar chart showing percentage adult fly viability assayed at 25 °C and 29 °C. Individual bars represent the mean viability ± S.E.M. of at least 4 independent experiments. Abbreviations: *pan-ms*, pan-muscular; *mes*, mesoderm; *ms*, larval muscles; *mn*, motor neurons; *n*, all CNS neurons except motor neurons. (**B–D**) In contrast to wild-type flies, escapers that have a global reduction in wmd (da-GAL4 > wmd-IR^{STARK}) exhibit wing defects similar to flies in which a wmd 5′ UTR mutant is balanced by a chromosomal deficiency that covers the wmd gene locus (wmd^{Matt}/Df[2R]BSC661). (**E**) Semi-quantitative RT-PCR of wmd and tbp-1 mRNA revealing that compared to control, flies with a ubiquitous wmd knockdown have a drastic reduction in the expression levels of wmd but not tbp-1 (housekeeping gene) mRNA transcripts. Abbreviation: RT, reverse transcriptase.

(Supplementary information, Fig. S3). Although the N-terminus varies in size across different species, it was found to be required for an efficient catalytic activity because it confers self-association properties (Boon et al., 2015). Tgs1 deletion results in embryonic or early pupal lethality in mouse (Jia et al., 2012) and *Drosophila* (Komonyi et al., 2005), respectively. These findings indicate that in contrast to the yeast *Saccharomyces cerevisiae* (Mouaikel et al., 2002), Tgs1 is most probably an essential gene in Metazoans. For confirmation, we employed an RNAi transgene (Tgs1-IR^{TAR}) targeting the coding sequence to deplete Tgs1 mRNA levels in *Drosophila* (Supplementary information, Fig. S2). A global reduction of Tgs1 via the ubiquitously expressing da-GAL4 driver results in adult lethality (Fig. 3A). To demonstrate RNAi specificity, through semi-quantitative RT-PCR analysis we first show that flies

have a drastic reduction in the expression level of *Tgs1* mRNA transcripts compared to controls (Fig. 3B). Secondly, lethality can be reverted on ubiquitous co-expression of a full-length *Tgs1* transgene (1032-GAL4 > Tgs1-IR^{TAR} + Tgs1^{FL}, 92% ± 10) but not RFP (1032-GAL4 > Tgs1-IR^{TAR} + mRFP, 0%). Aiming at determining whether different tissues have different requirements for Tgs1, we performed tissue-specific knockdown to test for an effect on adult viability. Notably, we find that lethality or reduced adult viability is the outcome if Tgs1 levels are reduced in either muscle tissue or the CNS. With regards to the latter, we note that a similar effect can be achieved if knockdown is restricted to motor neurons via the OK6-GAL4 driver (Fig. 3A). Overall, these studies imply that Tgs1 is required in both muscle and motor neurons to sustain the development of an adult viable organism.
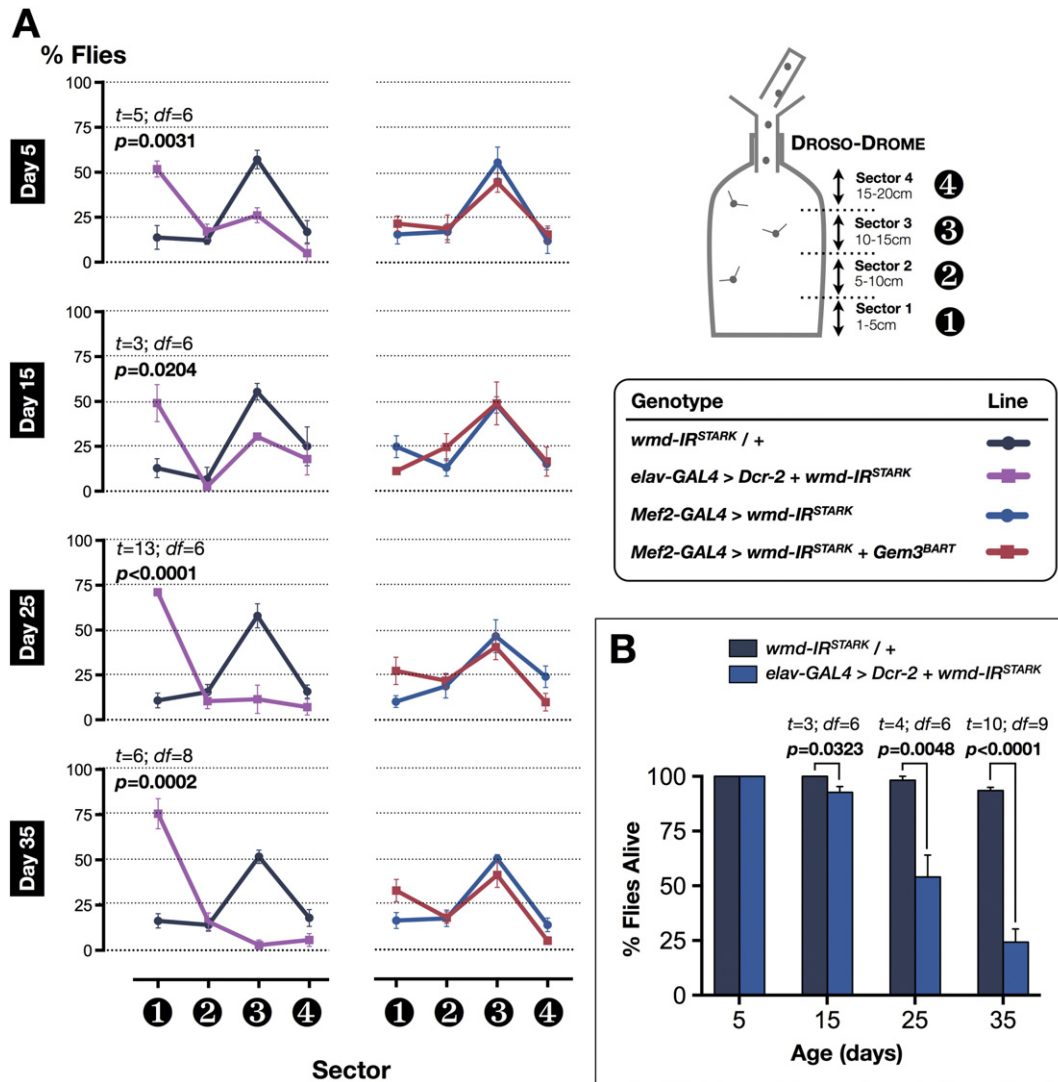
Fig. 2. Loss of wmd function in neurons has a progressive age-dependent negative effect on flight and adult survival. (A) *Left panel*: Enhanced RNAi-mediated knockdown of *wmd* in the CNS impairs flight performance as determined via the Droso-Drome apparatus, in which the height a fly falls determines its flight capacity. On day 5 and 15 post-eclosion, a significant percentage of organisms assessed were non-fliers, hence, they aggregate in sector 1, the lowest sector. The percentage number of organisms that are flight defective increases progressively with age. *Right panel*: Muscle-restricted knockdown of *wmd* does not enhance the flight defects associated with the ectopic expression of Gem3[BART]. (B) Percentage number of flies alive assessed at different time points during adulthood. Compared to the control, depletion of *wmd* in neurons results in a statistically significant decline in adult fly survival. In both (A) and (B), data presented are the mean ± S.E.M. of at least 4 independent experiments, and *n* ≥ 60 per genotype for each time point measured. Significance as tested by the unpaired *t*-test is indicated by the exact *p*-value. The *t*-statistic (*t*) and the associated degrees-of-freedom (*df*) are also given.

2.4. Tgs1 downregulation precipitates motor and viability defects associated with the Gem3[BART] hypomorph

We wished to investigate whether decreased levels of Tgs1 precipitate the motor system associated phenotypes of the *Gem3*[BART] hypomorph in a similar manner to that reported for members of the SMN-Gemins complex (Borg et al., 2015). To this end, we note that a 50% reduction in gene copy number via a chromosomal deletion (*Df(3R)Exel6178*) had no negative influence on flight performance when applied alone. However, in combination with the ectopic expression of Gem3[BART] in muscle tissue (*Mef2-GAL4 > Gem3*[BART] *+ Df(3R)Exel6178*), flies experienced an age-dependent progressive decline in motor performance starting at day 15 post-eclosion (Fig. 4A). To confirm that the deletion effect is specifically due to the *Tgs1* gene, we swapped the chromosomal deletion for an RNAi transgene. Although muscle-specific knockdown of Tgs1 alone (*Mef2-GAL4 > Tgs1-IR*[TAR]) has no negative influence, when combined with Gem3[BART] (*Mef2-GAL4 > Gem3*[BART] *+ Tgs1-IR*[TAR]), flies display flight defects that worsen progressively with age (Fig. 4A). Notably, we observed that when enhanced by augmented Dicer-2

levels, Tgs1 knockdown was sufficient to disrupt motor ability as well as adult survival in a progressive age-dependent manner (Fig. 4A, B). Overall, these findings are suggestive of a genetic interaction between *Tgs1* and *Gemin3*, and, importantly, reveal that Tgs1 is key for optimal motor performance.

2.5. Tgs1 overexpression is toxic in both Drosophila and yeast

In addition to a loss-of-function, we wanted to explore any defects arising as a result of a Tgs1 gain-of-function. Recently, we reported that muscle-specific overexpression of Gemin2 depressed normal motor function. Furthermore, its enhanced upregulation in all tissues had detrimental effects on viability, a phenotype that was conserved in the yeast *S. pombe* (Borg et al., 2015). Remarkably, we reveal an analogous outcome for Tgs1. In *Drosophila*, the ubiquitous expression of a full-length transgene in a wild-type background leads to lethality, a phenotype that can be reproduced if expression is restricted to muscle tissue (Fig. 3A). On further examination, we note that flies with a pan-muscular overexpression of Tgs1 fail to contract adequately during
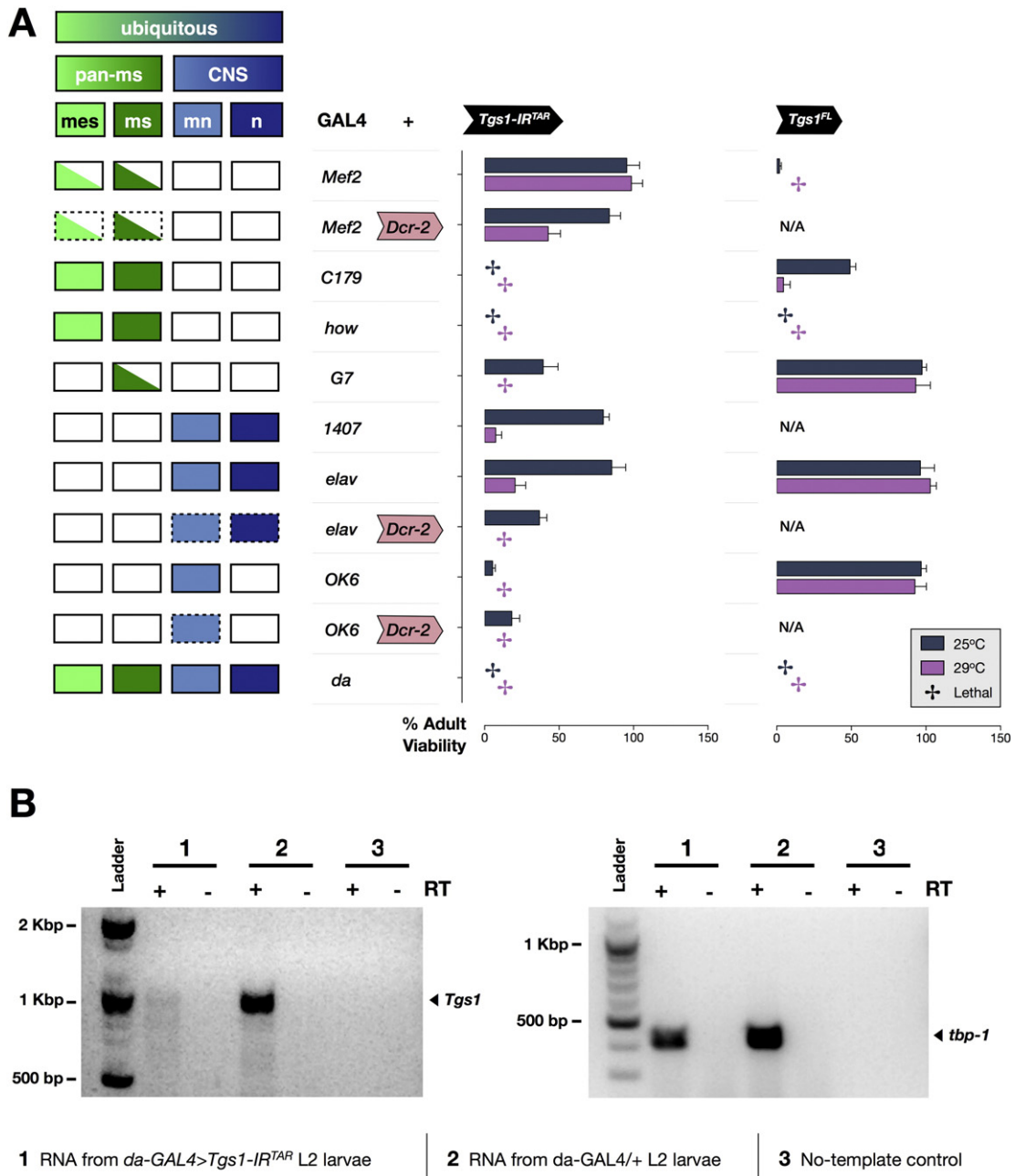
Fig. 3. Tgs1 function is indispensable for adult viability in either muscle or neurons. (**A**) Transgenic knockdown (*Tgs1-IR^{TAR}*) or overexpression (*Tgs1^{FL}*) of Tgs1 in all tissues via the ubiquitous *da*-GAL4 driver is lethal. Both genetic manipulations lead to a similar effect or reduced viability if expression is specifically directed to muscle. A deleterious effect is also observed on reduced Tgs1 levels in the CNS and can be replicated if expression is restricted to motor neurons. Results are more pronounced at temperatures that permit maximal GAL4 action (29 °C) and/or in an enhanced Dicer-2 background. *Left panel*: Tissue expression pattern of GAL4 drivers. *Right panel*: bar chart showing percentage adult fly viability assayed at 25 °C and 29 °C. Individual bars represent the mean viability ± S.E.M. of at least 4 independent experiments. Abbreviations: *pan-ms*, pan-muscular; *mes*, mesoderm; *ms*, larval muscles; *mn*, motor neurons; *n*, all CNS neurons except motor neurons; N/A, not available. (**B**) Semi-quantitative RT-PCR of *Tgs1* and *tbp-1* mRNA showing that compared to control, flies with a ubiquitous *wmd* knockdown have a drastic reduction in the expression levels of *Tgs1* but not *tbp-1* mRNA transcripts. Abbreviation: RT, reverse transcriptase.

pupariation as reflected by a significant difference in the puparial axial ratio when compared to the control genotype (Fig. 7C). We note that this phenotype, which mimics that described previously following disruption of SMN, Gemin2 or Gemin3 (Borg and Cauchi, 2013; Borg et al., 2015; Cauchi et al., 2008; Grice and Liu, 2011; Timmerman and Sanyal, 2012), is the consequence of a significant decrease in the rate of body wall muscle contractions during the third instar larval stage (Fig. S4).

In yeast, wild-type cells that were transformed with a plasmid carrying *SpTgs1* with or without a GFP tag under the control of a very strong *nmt1* promoter and, grown at 25 °C, displayed growth defects compared to control cells transformed with an empty plasmid (Fig. 5A, upper panel). The result is more pronounced in cells carrying a temperature-degron *Smn* (*tdSmn*) allele (Fig. 5A, lower panel), which is known to mimic the snRNP assembly and splicing defects observed in SMN deficient metazoan cells (Campion et al., 2010). At a temperature of 25 °C, Smn function is already disrupted in *tdSmn* cells as shown by a slow growth phenotype (Campion et al., 2010). Notably, we find that the overexpression of GFP has no negative influence on the growth rate of wild-type and *tdSmn* cells, thereby underlining the specificity of the Tgs1 gain-of-function phenotype. On inspection, Tgs1 overexpressing cells appear distended and more elongated compared to controls possibly indicating a problem in cell cycle progression (Fig. 5B). Importantly, this cellular phenotype as well as the decrease in viability following
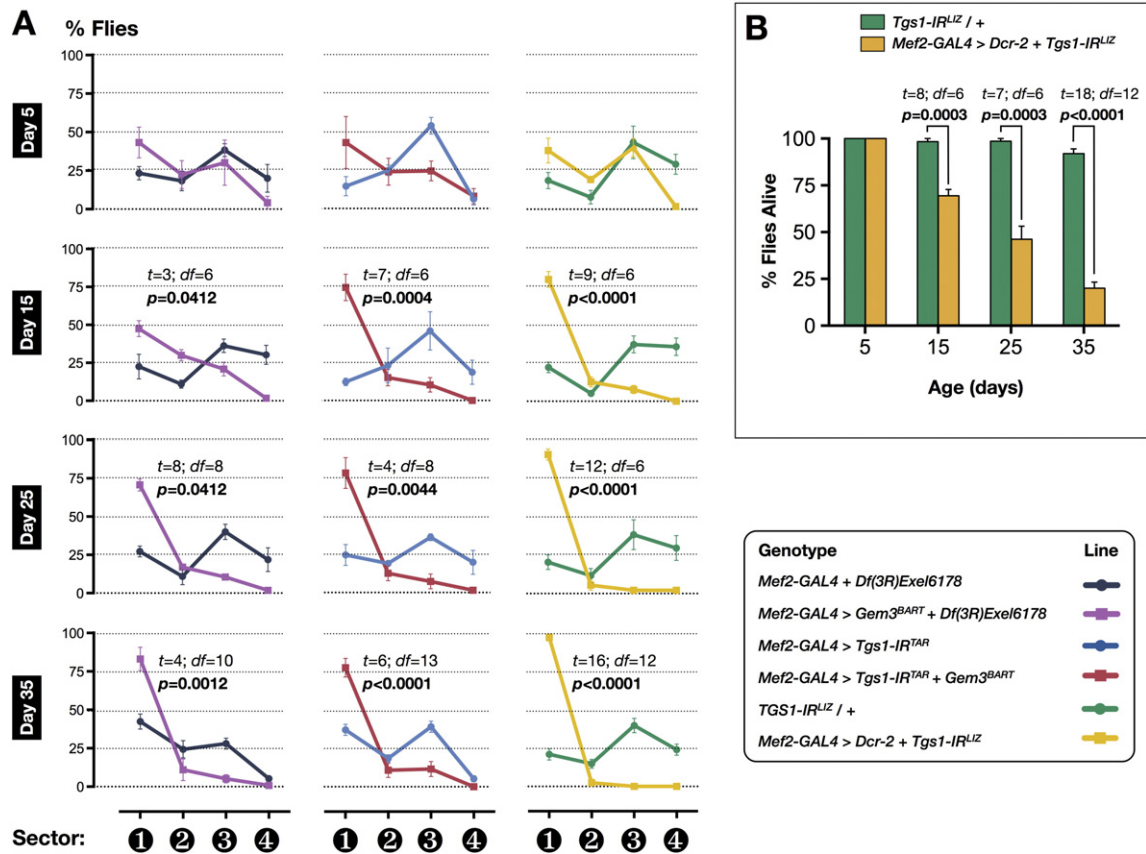
Fig. 4. A reduction in the Tgs1 gene copy number or Tgs1 knockdown expose motor defects associated with the Gem3BART hypomorph. (**A**) *Left panel*: In a heterozygous *Tgs1* deficient background brought about by a chromosomal deletion (*Df(3R)Exel6178*), the hypomorphic *Gem3BART* motor phenotype becomes apparent on day 15 post-eclosion and intensifies with age. *Middle Panel*: Analogous results are achieved if a *Tgs1* RNAi transgene is co-expressed with *Gem3BART* in muscle tissue. *Right panel*: Pan-muscular Tgs1 knockdown alone has a negative impact on flight only in the presence of extra levels of Dicer-2. (**B**) Boosted by extra Dicer-2 levels, Tgs1 knockdown also induces an age-dependent progressive decline in adult viability. In both (**A**) and (**B**), data presented are the mean ± S.E.M. of at least 4 independent experiments, and $n \geq 60$ per genotype for each time point measured. Significance as tested by the unpaired *t*-test is indicated by the exact *p*-value. The *t*-statistic (*t*) and the associated degrees-of-freedom (*df*) are also given.

upregulation of SpTgs1 is reminiscent of that previously observed in *S. pombe* Gemin2 overexpressors (Borg et al., 2015).

2.6. Muscle tissue is most adversely affected by deviations from normal pICln levels

Similar to Tgs1, pICln is a highly conserved snRNP biogenesis factor but unlike Tgs1, homology is not restricted to any particular region of the protein (Supplementary information, Fig. S5). The fly's orthologue amino acid sequence shows 11.72% identity and 49.82% similarity to that of human protein. Although pICln has been highly characterised in several biochemical and structural studies (Chari et al., 2008; Grimm et al., 2013; Pu et al., 1999), its functional dissection *in vivo* has been quite limited. In the yeast *S. pombe* we have recently shown that pICln is important for optimal cell growth although it is not an essential gene (Barbarossa et al., 2014). The situation is different in the mouse where its disruption causes early embryonic lethality (Pu et al., 2000). We wanted to first investigate whether the same holds true for *Drosophila*. To this end, we find that lethality is the endpoint of a global knockdown of pICln through the ubiquitous expression of an RNAi transgene (*pICln-IR^RAD*) targeting the majority of pICln's coding sequence (Fig. 6A; Supplementary information, Fig. S2). RNAi specificity was tested through rescue of lethality on ubiquitous co-expression of a full-length *pICln* transgene (*da-GAL4 > pICln-IR^RAD + pICln^FL*, 39% ± 10). Lethality was not reverted when a GFP transgene was used instead (*da-GAL4 > pICln-IR^RAD + EGFP*, 0%), hence, eliminating the possibility that rescue is the result of GAL4 dilution effects induced by multiple UAS-constructs in the background. Furthermore, through semi-

quantitative RT-PCR analyses, we provide evidence of a profound depletion of *pICln* transcript levels on RNAi-mediated knockdown compared to controls (Fig. 6B). Interestingly, pICln function can be disrupted by enhanced protein levels delivered through the ubiquitous expression of a pICln transgene (Fig. 6A). In this respect, wild-type flies overexpressing pICln in all tissues are never adult viable, a situation that is comparable to that of Gemin2 (Borg et al., 2015) and Tgs1 (above). Attempting to investigate which tissue is most vulnerable to a change in protein levels, we restricted pICln disruption to either muscle or neurons. We find that adult viability is most adversely impacted if knockdown or overexpression of pICln is specifically limited to muscle tissue (Fig. 6A). On closer examination of flies with a strong muscle-specific overexpression of pICln (*how-GAL4 > pICln^FL*), we observed that similar to Tgs1 overexpressors (above) their puparia have abnormal axial ratios indicating an unsuccessful attempt at contracting adequately during pupariation (Fig. 7C). Flies perish during pupation. Overall these findings indicate that pICln is an essential gene in *Drosophila* and tightly regulated protein levels are important for its optimal function within muscles.

2.7. pICln overexpression affects motor function and in combination with Gem3BART leads to lethality

Unexpectedly, we noticed that flies overexpressing full-length pICln in a pan-muscular expression pattern via the moderately strong *Mef2*-GAL4 driver displayed motor system defects during adulthood. As early as day 5 post-eclosion, flies were flightless compared to controls (Fig. 7A). Furthermore, they exhibit wing posture defects, including
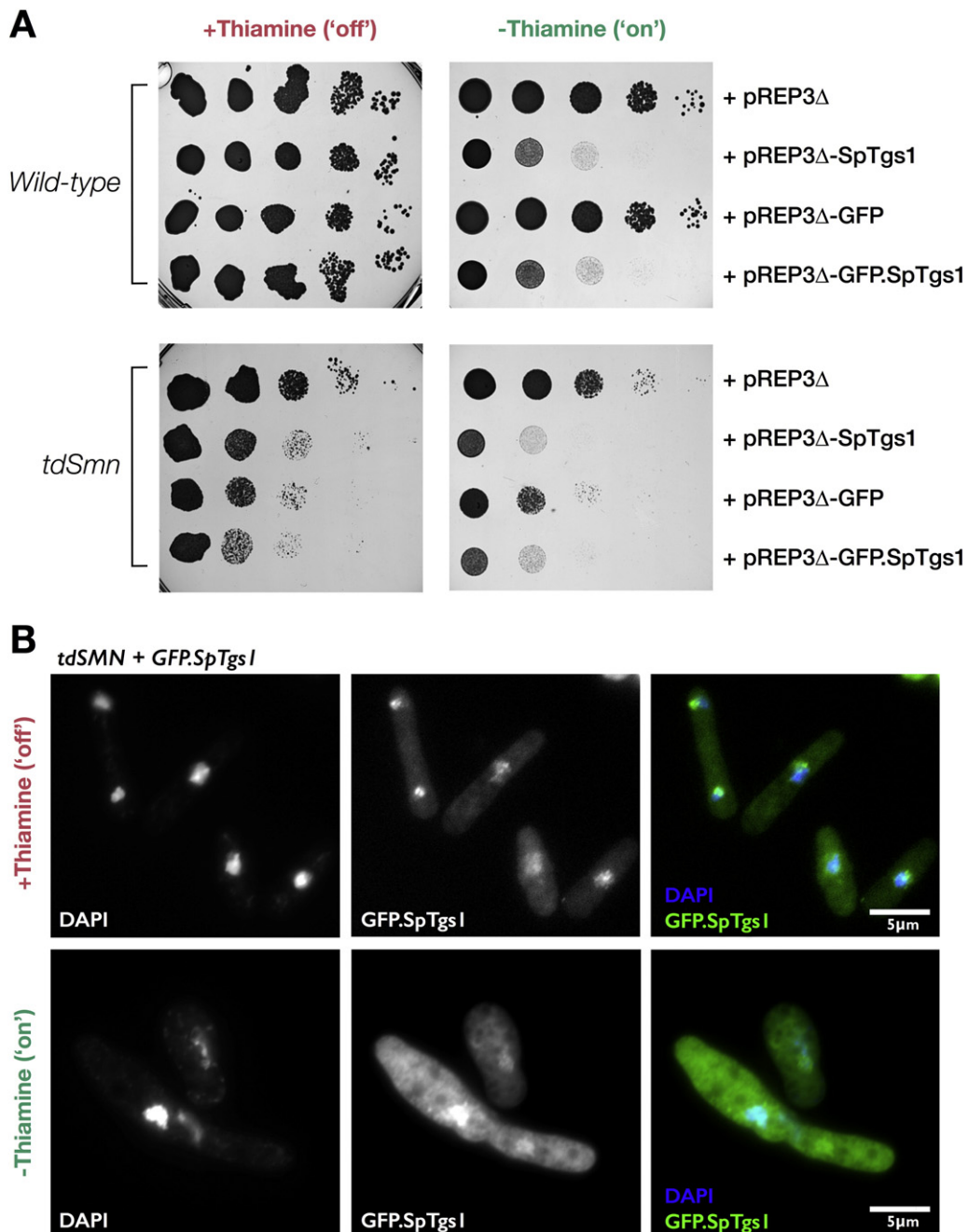
Fig. 5. Tgs1 overexpression has deleterious effects on cell viability in *S. pombe*. (**A**) Wild-type (upper panel) or *tdSmn* (lower panel) cells were transformed with the pREP3Δ plasmid that was either empty or carrying the *S. pombe Tgs1* gene with or without a GFP tag, or the *GFP* gene alone. Cultures of comparable density were then serially diluted, spotted on EMM2–Leu plates in the presence (expression is repressed) or absence (expression is induced) of Thiamine and incubated at 25 °C for 5 days to test for their growth ability. In a wild-type background, *nmt1*-promoter driven overexpression of SpTgs1 or GFP·SpTgs1 but not GFP induces growth defects. The phenotype is more pronounced in a *tdSmn* background. (**B**) In addition to an increased GFP signal, cells overexpressing the GFP·SpTgs1 fusion protein lose the rod-shaped morphology that is typical in controls, hence, appearing distended and elongated.

droopy wings when compared to controls in which wings typically run dorsal and parallel to the body (Fig. 7B). Importantly, flight defects were reverted when pICln overexpression was combined with an RNAi transgene targeting pICln, presumably due to restoration of pICln levels to the normal range. The same result cannot be obtained if the RNAi transgene is exchanged for a GFP transgene, thereby excluding the possibility that rescue is due to GAL4 dilution effects (Fig. 7A). pICln knockdown enhanced by heightened Dicer-2 levels also gives rise to flight defects, which indicates that a decrease is as deleterious as an increase in pICln levels. In confirmation, we note that flies with either an enhanced depletion or an overexpression of pICln, which were monitored for 24 h or more display similar locomotor defects when they are awake (Fig.

S6). Finally, we probed for an *in vivo* association between pICln and Gemin3. In this regard, synthetic lethality is the endpoint when pICln is overexpressed together with Gem3[BART] in muscle tissue. In summary, we expose a genetic interaction between pICln and Gemin3, and demonstrate that deviations from the normal range of pICln levels have unfavourable effects on the motor system.

2.8. Toxicity of pICln overexpression is conserved in S. pombe and involves cytoplasmic Sm protein retention

Based on elegant molecular and structural studies, pICln and Gemin2 are thought to have remarkably similar roles within their respective
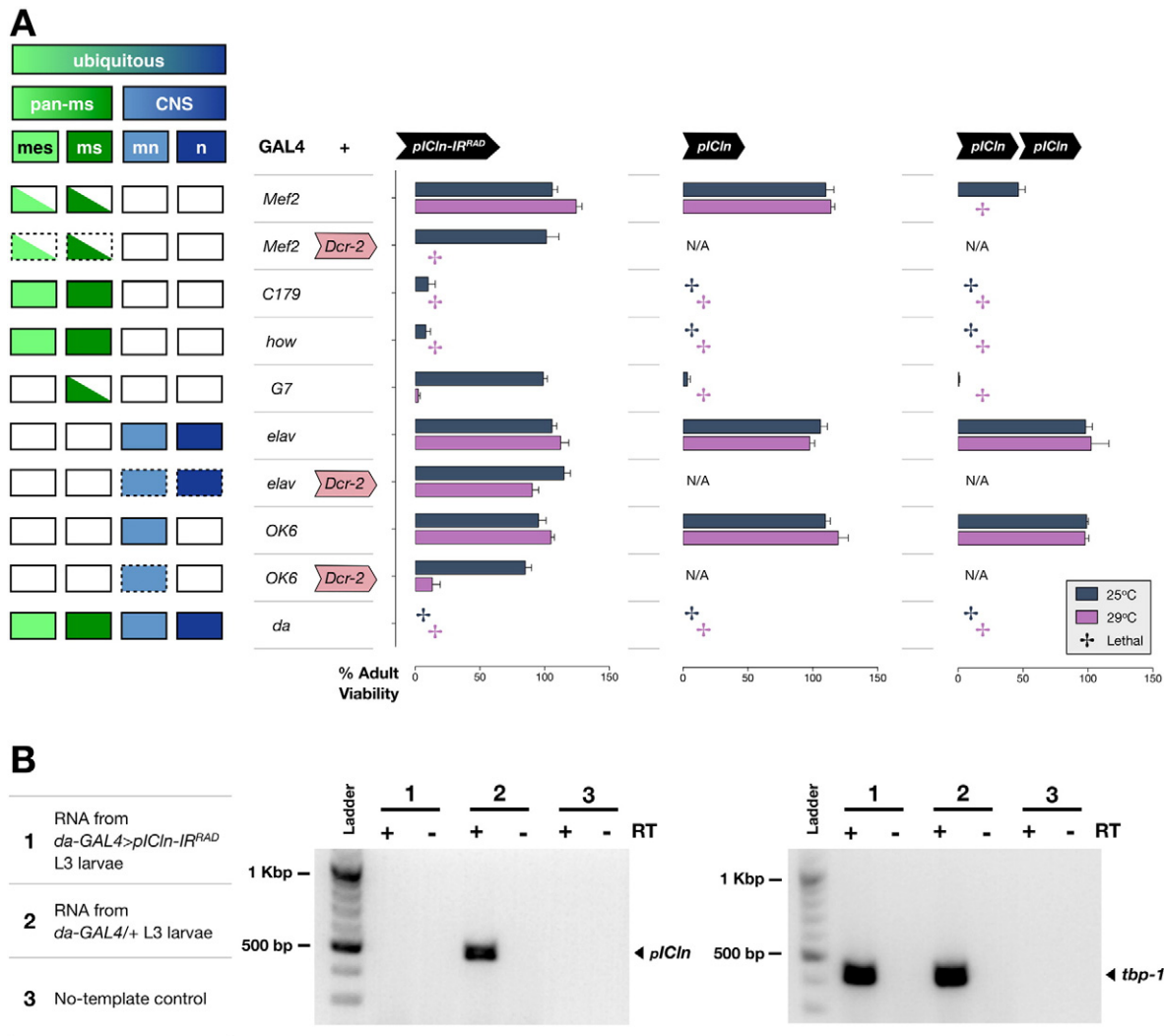
Fig. 6. Deviations from normal pICln levels in muscle have a negative influence on adult viability. (A) pICln levels were decreased by RNAi-mediated knockdown (*pICln-IR^{RAD}*) and increased by the overexpression of a single or double dose of a full-length *pICln* transgene. All three genetic manipulations have a negative impact on adult viability when individually directed to either all tissues or selectively to muscle tissue. Results are stronger in an enhanced Dicer-2 background, in case of knockdown, and/or at temperatures that permit maximal GAL4 action (29 °C). *Left panel*: Tissue expression pattern of GAL4 drivers. *Right panel*: bar chart showing percentage adult fly viability assayed at 25 °C and 29 °C. Individual bars represent the mean viability ± S.E.M. of at least 4 independent experiments. Abbreviations: *pan-ms*, pan-muscular; *mes*, mesoderm; *ms*, larval muscles; *mn*, motor neurons; *n*, all CNS neurons except motor neurons; N/A, not available. (B) Semi-quantitative RT-PCR of *pICln* and *tbp-1* mRNA showing that compared to control, flies with a ubiquitous *pICln* knockdown have a strong reduction in the expression levels of *pICln* but not *tbp-1* mRNA transcripts. Abbreviation: RT, reverse transcriptase.

complexes. Both proteins hug an Sm protein subset that is organised into the same spatial configuration found in the assembled Sm ring (Chari et al., 2008; Grimm et al., 2013; Zhang et al., 2011). Given that disruption of both proteins *in vivo* gives rise to intriguingly similar phenotypes, we asked whether pICln's responsible mechanism is similar to the one we recently described in *S. pombe* for Gemin2 (Borg et al., 2015). To this end, we first show that pICln overexpression has detrimental consequences also in yeast. Indeed, in wild-type cells, the expression of *SpICln* under the control of a very strong *nmt1* promoter results in growth defects. These are more dramatic in a *tdSmn* background but were absent in negative controls including cells transformed with an empty plasmid or *SpSmn* overexpressors (Fig. 8A).

To investigate the subcellular distribution of Sm proteins in pICln overexpressing cells, we double transformed cells with plasmids carrying *SpICln* and *GFP·SmB* that were under the control of a very strong and a medium strong *nmt1* promoter, respectively. The growth defects associated with SpICln upregulation persisted even in the presence of enhanced levels of SmB (Fig. 8B). We observed that pICln overexpressors accumulated higher levels of SmB in the cytoplasm in contrast to control cells in which SmB was, as expected (Bordonne, 2000), mostly localised

to the nucleus (Fig. 8C). Quantification of the GFP·SmB fluorescence signal revealed that SmB is mislocalised to the cytoplasm. In this regard, compared to the control genotype, cells overexpressing pICln had lower and higher levels of SmB in the nucleus and cytoplasm, respectively (Fig. S7). Furthermore, cells with heightened levels of pICln are, on average, more than two times longer compared to controls (Fig. 8C and Fig. S8), a phenotype that is thought to be due to blockage or delay in cell cycle progression. These findings reveal that similar to Gemin2 (Borg et al., 2015), disruption of pICln results in a surplus of Sm proteins within the cytoplasm, most likely indicating a cytoplasmic block in the snRNP assembly pathway.

2.9. A physical association between Gemin3 and Tgs1 or pICln

Genetic interactions represent functional relationships between genes that are identified by comparing the effect of disrupting each gene individually to the effect of disrupting both genes simultaneously. We have recently described genetic interactions between Gemin3 and core members of the *Drosophila* SMN-Gemins complex (Borg et al., 2015). Most of these interactions were identified as being also physical
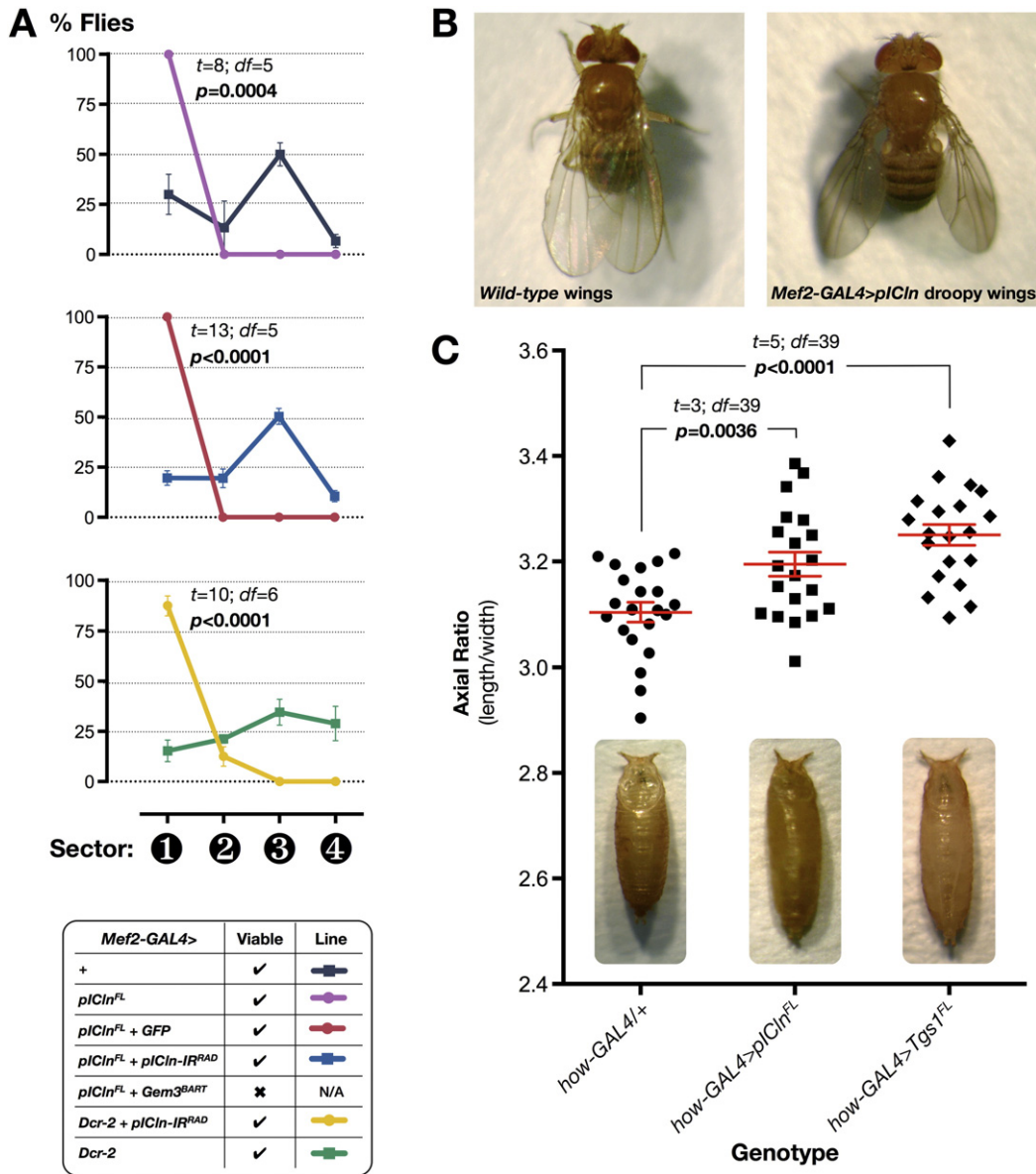
Fig. 7. pICln disruption leads to motor, wing posture and puparial defects. (**A**) Compared to controls (*Mef2-GAL4/+),* flies with a pan-muscular overexpression of full-length pICln (*Mef2-GAL4 > pICln^{FL}*) are entirely flightless. The phenotype persists in the presence of GFP (*Mef2-GAL4 > pICln^{FL} + GFP*) but it is rescued by co-expression of an RNAi construct (*Mef2-GAL4 > pICln^{FL} + pICln-IR^{RAD}*). The combined overexpression of pICln and Gem3^{BART} is lethal indicating a genetic interaction between *pICln* and *Gemin3*. In contrast to the control genotype (*Mef2-GAL4 > Dcr-2*), flies with an enhanced knockdown of pICln (*Mef2-GAL4 > Dcr-2 + pICln-IR^{RAD}*) are also non-fliers in their majority. Data presented are the mean ± S.E.M. of at least 3 independent experiments at day 5 post-eclosion, and $n \geq 60$ per genotype. Significance as tested by the unpaired t-test is indicated by the exact p-value. The t-statistic (t) and the associated degrees-of-freedom (df) are also given. (**B**) Flies with muscle-restricted pICln overexpression develop droopy wings instead of the dorsal wing posture that is typical in wild-type flies. (**C**) *Bottom*, Puparia of flies with a strong pan-muscular overexpression of pICln (*how-GAL4 > pICln^{FL}*), Tgs1 (*how-GAL4 > Tgs1^{FL}*) and the GAL4 driver control (*how-GAL4/+*). *Top*, Chart showing that pICln or Tgs1 overexpressors have a significantly larger puparial axial ratio when compared to the control genotype. The mean is marked by a horizontal line running through the data points and error bars are ±S.E.M. Significance as tested by the unpaired t-test is indicated by the exact p-value. The t-statistic (t) and the associated degrees-of-freedom (df) are also given. $n = 21$ for *how-GAL4/+*, $n = 20$ for *how-GAL4 > pICln^{FL}*, and $n = 20$ for *how-GAL4/Tgs1^{FL}*.

in earlier studies (Cauchi et al., 2008; Guruharsha et al., 2011; Kroiss et al., 2008; Sen et al., 2013; Shpargel et al., 2009). In this context, we asked whether the genetic interactions we have identified between *Gemin3* and *wmd/Unrip*, *Tgs1* or *pICln* (summarised in Fig. 9A) translate into physical interactions between the respective proteins. To this end we tested for association in the yeast two-hybrid assay. SMN, Tgs1, pICln and wmd/Unrip were fused to the GAL4 DNA binding domain (GAL4-BD) to use as bait whereas Gemin3 was fused to the GAL4 activation domain (GAL4-AD) to use as prey. Both bait and prey plasmids were then transformed into the respective yeast strain and following mating, diploids containing both plasmids were screened for protein-protein interaction. The combination of GAL4-AD fused to Gemin3 and GAL4-BD fused to SMN served as the positive control while a GAL4-BD vector

without an insert (empty) was used as the negative control. *In vivo* interactions were obtained for Gemin3 and SMN, Tgs1, or pICln as the yeast strain containing the respective bait and prey fusions were able to grow on –Leu–Trp–His selective plates (Fig. 9B). However, Gemin3 does not interact physically with wmd/Unrip as shown by the absence of growth. Positive interactions including Gemin3–SMN, Gemin3–pICln and Gemin3–Tgs1, in the order of decreasing strength, were confirmed on quantitation via the β-galactosidase assay (Fig. S9).

3. Discussion

Making use of the *Drosophila* model, in the present study, we first determined that although loss of wmd/Unrip triggers motor
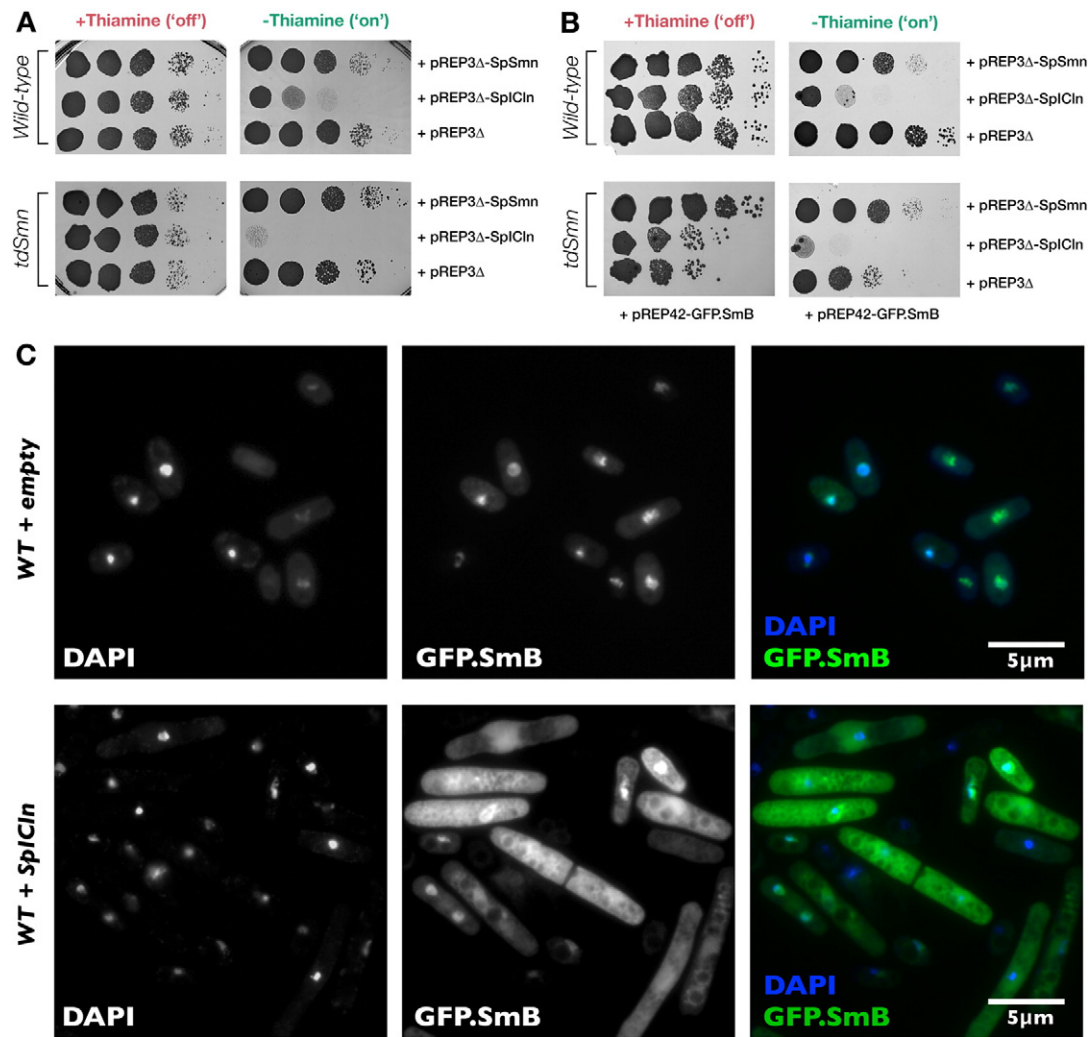
Fig. 8. pICln overexpression is toxic in *S. pombe* through a mechanism that involves retention of Sm proteins in the cytoplasm. (**A**) Cells transformed with the pREP3Δ vector carrying the *S. pombe* pICln gene displayed growth defects in contrast to cells that were transformed with the pREP3Δ plasmid, which was either empty or carrying the *S. pombe* Smn gene, both of which serving as a negative control. Effects are stronger in a *tdSmn* background. Cultures of comparable density were serially diluted, spotted on EMM2–Leu plates in the presence (expression is repressed) or absence (expression is induced) of Thiamine and incubated at 25 °C for 5 days. (**B**) Wild-type or *tdSmn* cells were transformed with a plasmid carrying GFP·SmB in combination with the plasmids indicated on the right. Cultures of comparable density were then serially diluted, spotted on EMM2–Leu–Ura- plates in the presence (expression is repressed) or absence (expression is induced) of Thiamine and incubated at 25 °C for 5 days to examine their growth ability. The growth defect of either wild-type or *tdSmn* cells overexpressing pICln persist in the presence of increased levels of SmB. (**C**) In GFP·SmB-expressing wild-type cells, SmB is predominantly localised to the nucleus. On upregulation of pICln, SmB accumulates in the cytoplasm and cells exhibit an elongated phenotype.

dysfunction, a functional relationship or a direct association with the key SMN-Gemins complex member Gemin3 could be ruled out. Secondly, we reveal that disruption of the pivotal snRNP biogenesis factors Tgs1 and pICln leads to phenotypes that mirror those previously uncovered on loss of SMN-Gemins complex components. Supported by a strong genetic interaction and a physical association between both factors and Gemin3, we strengthen the evidence linking appropriate snRNP biogenesis to optimal motor system function.

3.1. Drosophila Unrip: in or out?

It has been proposed that SMN and Gemin2 form the ancestral core of the SMN-Gemins complex, which increased its complexity in evolution through the addition of several apparently diverse proteins including Gemins 3–8 and Unrip (Cauchi, 2010; Kroiss et al., 2008). Although Unrip is thought to latch on the SMN-Gemins complex via an association with Gemin7, it does so only weakly (Otter et al., 2007) and in a compartment-specific manner (Grimmler et al., 2005). It thus remains unclear whether Unrip can be considered as a steady member of the SMN-Gemins complex despite reports underscoring its requirement

for efficient snRNP assembly *in vitro* (Carissimi et al., 2005; Grimmler et al., 2005; Ogawa et al., 2009). Our *in vivo* investigations suggest that wmd, the *Drosophila* Unrip orthologue, is required in the motor system for adult viability and normal motor performance, a finding which parallels that reported for all SMN-Gemins complex members (Borg and Cauchi, 2013; Chang et al., 2008). However, we failed to detect a functional relationship between Gemin3 and wmd/Unrip whereas in an earlier study, we were able to do so between Gemin3 and all the other members of the SMN-Gemins complex (Borg et al., 2015).

In view of our findings, it is plausible that wmd/Unrip is not a core complex member in *Drosophila* and is involved in roles that are unrelated to snRNP biogenesis. The absence of Gemin7 in *Drosophila* (Cauchi, 2010), a complex component that serves as the Unrip recruiter in vertebrates including humans lends further support to this hypothesis. Furthermore, compared to the human homologue, wmd has a level of amino acid conservation (identity) that is quite high (55%) and is therefore incongruous with that of the constituent members of the *Drosophila* SMN-Gemins complex (Smn, 21%; Gem2, 25%; Gem3, 17%; Gem5, 14%). It is noteworthy that in vertebrates, Unrip was initially identified as a transforming growth factor-β (TGF-β) receptor-interacting protein
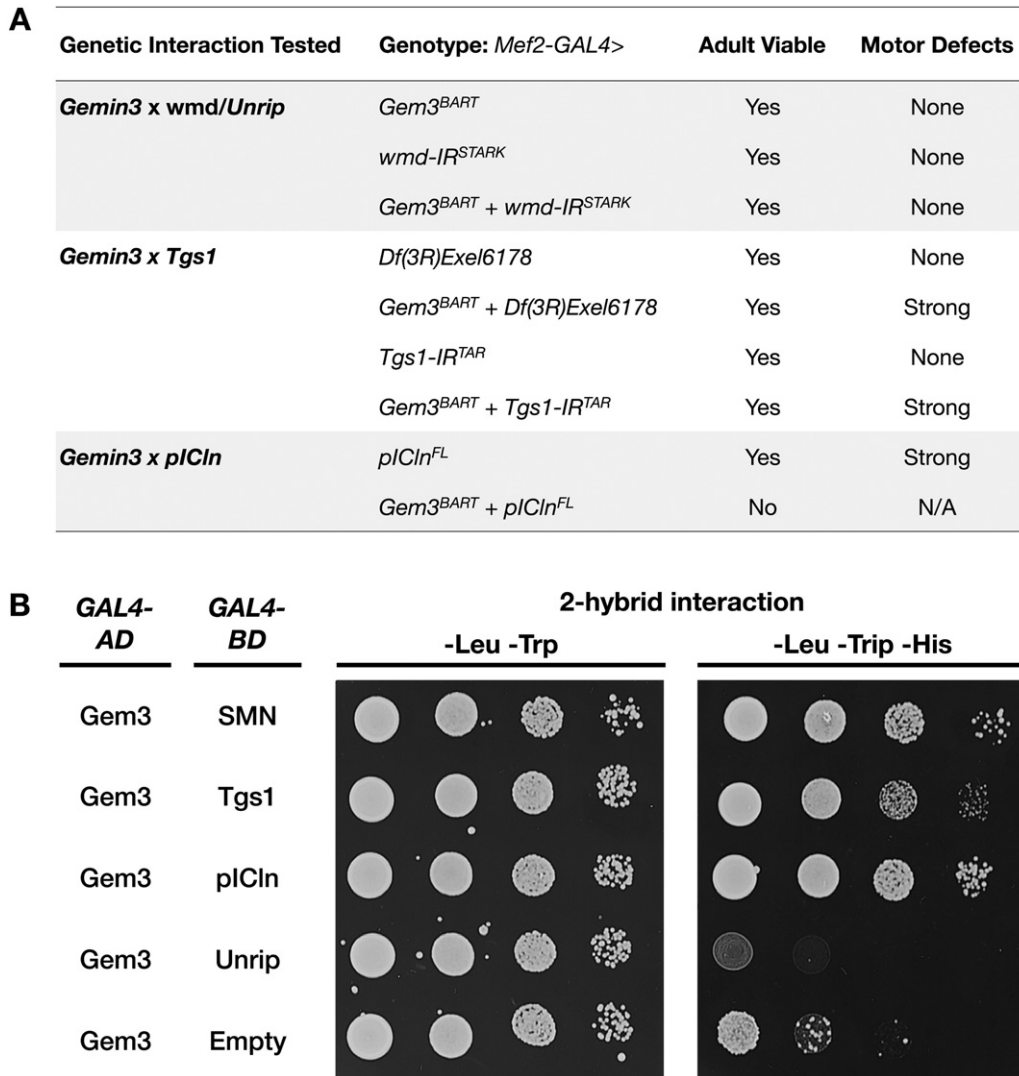
A

Genetic Interaction Tested	Genotype: *Mef2-GAL4>*	Adult Viable	Motor Defects
Gemin3* x wmd/*Unrip	*Gem3*[BART]	Yes	None
	wmd-IR[STARK]	Yes	None
	Gem3[BART] + *wmd-IR*[STARK]	Yes	None
Gemin3* x *Tgs1	*Df(3R)Exel6178*	Yes	None
	Gem3[BART] + *Df(3R)Exel6178*	Yes	Strong
	Tgs1-IR[TAR]	Yes	None
	Gem3[BART] + *Tgs1-IR*[TAR]	Yes	Strong
Gemin3* x *pICln	*pICln*[FL]	Yes	Strong
	Gem3[BART] + *pICln*[FL]	No	N/A

B

GAL4-AD	GAL4-BD	2-hybrid interaction
		-Leu -Trp / -Leu -Trip -His
Gem3	SMN	
Gem3	Tgs1	
Gem3	pICln	
Gem3	Unrip	
Gem3	Empty	

Fig. 9. **Genetic interactions between Gemin3 and Tgs1 or pICln translate into physical interactions.** (**A**) Summary of the genetic interactions uncovered in this study through synthetic enhancement or lethality. (**B**) The reporter strain carrying yeast two-hybrid plasmids expressing the indicated proteins was spotted in serial dilutions on –Leu–Trp, or –Leu–Trp–His plates. Growth on –Leu–Trp–His plates indicate a positive interaction between Gemin3 and SMN, Tgs1, or pICln but not between Gemin3 and wmd/Unrip. At least 3 independent experiments were performed, and the result of one representative is shown.

that is a negative regulator of TGF-β signalling (Datta et al., 1998). This finding was followed by a flurry of reports that delineate its role under the Strap alias as a regulator of cell proliferation and cell death through the modulation of several other signalling pathways (reviewed in Reiner and Datta, 2011). These findings underscore the important cellular functions of Unrip outside the SMN-Gemins complex and raise the possibility that Unrip gained SMN-Gemins complex membership only later on during evolution.

3.2. A strengthened link between snRNP biogenesis and optimal motor function

SMN and its associates have been implicated in several cellular processes that could be relevant to SMA but in view of sizeable evidence, what stands out is the link between altered snRNP production and motor system dysfunction. First, levels of SMN strongly dictate the capacity of cell extracts to produce snRNPs (Wan et al., 2005), which in turn influences SMA phenotypic severity (Gabanella et al., 2007) or phenotypic rescue in the murine SMA model (Workman et al., 2009). Second, maximal snRNP assembly activity in the spinal cord coincides with the highest exigencies of SMN during the development of the motor unit (Foust et al., 2010; Gabanella et al., 2005; Kariya et al.,

2014; Le et al., 2011; Lutz et al., 2011). Third, signature transcriptome abnormalities that are thought to contribute to the collapse of the motor system in the disease have been identified *in vivo* (Imlach et al., 2012; Lotti et al., 2012; Zhang et al., 2013). Finally, restoration of normal snRNP levels through either injection of purified snRNPs or the introduction of the *SMN*[A111G] allele, which is capable of snRNP assembly, corrects the disease phenotype in zebrafish (Winkler et al., 2005) and mouse SMA models, respectively (Workman et al., 2009). Our study fits into this context by showing that pICln and Tgs1, two factors that have a starring role in the respective early and late phase of snRNP assembly, are required in the motor system for adult viability and optimal motor performance. Importantly, we show that depletion of either factor gives rise to phenotypes that are remarkably similar to those described on loss of SMN or Gemins (Borg and Cauchi, 2013; Borg and Cauchi, 2014; Borg et al., 2015; Cauchi et al., 2008; Chang et al., 2008; Rajendra et al., 2007). These findings are in line with those of Winkler et al. (2005) who described similar motor system degeneration phenotypes following the silencing of SMN, Gemin2 or pICln expression in zebrafish embryos.

Surprisingly, we find that in addition to knockdown, the overexpression of either Tgs1 or pICln is detrimental to the motor system, a situation reminiscent of that uncovered for Gemin2 (Borg et al., 2015).

Toxicity is conserved in the yeast *S. pombe*, where we show that SpICln overexpression induces a surplus of Sm proteins within the cytoplasm and decreased levels in the nucleus. This mechanism is analogous to that reported in HeLa cells for the dominant-negative mutant SMNΔN27 (Pellizzoni et al., 1998) or Gemin2 overexpression in *S. pombe* (Borg et al., 2015), and most likely indicates a cytoplasmic block in snRNP biogenesis. Corroborating these results, injection of high concentrations of pICln in *Xenopus* oocytes was found to inhibit nuclear import of snRNPs (Pu et al., 1999). It is thought that Sm proteins bound to pICln are prevented from binding to RNA (Chari et al., 2008; Pu et al., 1999), a condition that is likely to backfire, when levels of pICln are exorbitantly high. Hence, an overabundance of pICln could hijack Sm proteins, consequently impeding the progression of the snRNP assembly reaction. To our knowledge, neither Tgs1 nor pICln have been directly linked to axonal transport, which is considered as the leading non-canonical function of the SMN-Gemins complex (Fallini et al., 2012). Conversely, an extensive number of studies highlight the critical role of both factors in snRNP biogenesis. Notably, HeLa cells depleted of TGS1 or SMN reduces the nuclear portion of snRNPs (Lemm et al., 2006), and *Tgs1* deletion in either yeast (Mouaikel et al., 2002) or *Drosophila* (Komonyi et al., 2005) was found to disrupt TMG cap formation. In case of pICln, the *Drosophila* orthologue permitted structural studies that established a key role for pICln in the formation of higher-order Sm subassemblies and mechanistic insights into how Sm proteins are handover to the SMN-Gemins complex (Chari et al., 2008; Grimm et al., 2013). Furthermore, we have recently shown that loss of *pICln* in yeast gives rise to a reduction in snRNP levels and inefficient splicing (Barbarossa et al., 2014).

We believe that the similar phenotypic outcomes following disruption of Tgs1, pICln or any member of the SMN-Gemins complex point to the participation of these factors in a common or shared pathway. Our view is strengthened by evidence of a strong functional relationship and a physical interaction between Gemin3 and either Tgs1 or pICln. Hence, it is tempting to speculate that the involvement of the SMN-Gemins complex in snRNP biogenesis is key to guard against motor system dysfunction and it is this role that is perturbed in SMA. It is interesting to note that snRNPs were also found to be mislocalised to the cytoplasm in cells derived from amyotrophic lateral sclerosis (ALS) patients with pathogenic mutations in the nuclear protein FUS (Gerbino et al., 2013; Yu et al., 2015). Considering the intersection of the SMN-Gemins complex with ALS (reviewed in Cauchi, 2014), the most common motor neuron disease of adulthood, our findings have broader implications on our understanding of the mechanisms underpinning degenerative motor neuron disorders.

4. Materials & methods

4.1. Fly stocks

Flies were cultured on standard molasses/maizemeal and agar medium in plastic vials at an incubation temperature of 25 °C unless otherwise stated. Wild-type strain was *Oregon R*. Expression of inducible transgenes was performed via the GAL4/upstream activation sequence (UAS) system (reviewed in Cauchi and van den Heuvel, 2006). The *wmd* transposon insert line, *wmd^Matt* (P[SUPor-P]wmd^KG07581), the chromosomal deletions covering either *wmd* (Df[2R]BSC661) or *Tgs1* (Df[3R]Exel6178), and the fluorescent protein transgenes (*UAS.EGFP* and *UAS.dsRed*) were obtained from the Bloomington *Drosophila* Stock Center (NIH P40OD018537) at Indiana University, USA. The RNAi transgenic constructs, *UAS.wmd-IR^STARK* (106171) and *UAS.Tgs1-IR^TAR* (29503), were obtained from Vienna *Drosophila* Resource Center, Austria (Dietzl et al., 2007). The RNAi transgenic constructs, *UAS.Tgs1^LIZ* (31241R-3) and *UAS.pICln^RAD* (4924R-3), were acquired from the National Institute of Genetics Fly Stock Center, Japan. The full-length *Tgs1* (*UAS.Tgs1^FL*) transgene was obtained from the FlyORF Zurich ORFeome Project, Switzerland (Bischof et al., 2013). The *Gem3^BART* allele was

described and characterised previously (Borg et al., 2015). The provenance of the GAL4 lines utilised in this study was detailed previously (Borg and Cauchi, 2013; Cauchi et al., 2008). Combination of the various genetic tools including alleles, transgenes, and GAL4 lines was carried out according to standard genetic crossing schemes.

4.2. Yeast strains

The *S. pombe* strain carrying the *tdSmn* allele has been characterised previously (Campion et al., 2010). Cells were grown on YES or minimal EMM2 medium with adequate supplements. To control plasmid expression, cells were cultured on EMM2–Leu–Ura plates and Thiamine was used to switch expression either 'on' (absence) or 'off' (presence). Standard methods were used for both growth and genetic manipulations (Moreno et al., 1991).

4.3. Drosophila transgenic constructs

The generation of the *UAS.pICln^FL* transgenic construct involved the PCR-amplification of the full coding sequence of pICln, and ligation via the *Not*I and *Kpn*I restriction sites of the pUAST vector. The cDNA clone for pICln (SD10511) was obtained from the *Drosophila* Genomics Resource Centre (Indiana University, USA). Ligation products were used to transform NEB 10-beta competent *Escherichia coli* cells (New England Biolabs, Hitchin, UK) using standard protocols. Correct transformants were further propagated, and their harbouring plasmids were purified prior to microinjection in *w^1118* embryos.

4.4. S. pombe transgenic constructs

The fission yeast pICln gene was amplified from the *pREP41-N-TAP-SpICln* plasmid (Barbarossa et al., 2014). PCR products were cut with the *Bam*HI and *Xma*I restriction enzymes and cloned into the *S. pombe* pREP3Δ vector, a derivative of pREP3 harbouring the thiamine-repressible *nmt1* promoter (Maundrell, 1993). The generated plasmid was named *pREP3Δ-SpICln*. The GFP gene was amplified from the *pREP41-N-GFP* plasmid (Craven et al., 1998) as a blunt-*Sac*I fragment and cloned into pREP3Δ previously digested with *Bam*H1, blunt ended and cut with *Sac*I. The generated vector was named *pREP3Δ-GFP*. The SpTgs1 was PCR amplified from the pTN-RC5 cDNA library (a kind gift from T. Nakamura, YGRC, Osaka, Japan) as *Bam*HI–*Xma*I and *Sal*I–*Xma*I fragments which were cloned into vectors to generate the *pREP3Δ-SpTgs1* and *pREP3Δ-GFP·SpTgs1* plasmids, respectively. The construction of the *pREP3Δ-SpSmn* and *pREP42-GFP·SmB* plasmids was described previously (Borg et al., 2015). Plasmids were purified and confirmed by sequencing. Transformations were carried out according to standard techniques (Moreno et al., 1991).

4.5. Analysis of mRNA expression via semi-quantitative RT-PCR

RNA was extracted using the RNeasy kit (Qiagen Ltd., Manchester, UK) and then equal concentrations were reverse transcribed into cDNA using the M-MuLV Reverse Transcriptase (New England Biolabs, Hitchin, UK) following manufacturer's instructions. mRNA transcripts were PCR-amplified using primers specific to *wmd* (forward: 5′-ATCTCGGCCTGCAAAG-3′; reverse: 5′-TCTAGGCTGTTCGGATTGCT-3′), *Tgs1* (forward: 5′-TTGTGACGAGGAACAACAGC-3′; reverse: 5′-ACCATTCGGGTGTCCAGATA-3′), *pICln* (forward: 5′-ATTGCCCAAAACACGCTATC-3′; reverse: 5′-CATCCTCCTCCATAGCCTCA-3′), and *tbp-1* (forward: 5′-GACACTGCCCTACCTGGTGT-3′; reverse: 5′-GGTGAATGCCAAGGTTTTTG-3′). Conditions were chosen so that the end cycle was in the exponential phase of amplification. RT-PCR products were then separated by electrophoresis on a 1.5% agarose gel containing ethidium bromide and bands were visualised under ultraviolet light.

4.6. Viability, survival and growth assessment

Comparison of the viability and cell growth rate of different *S. pombe* strains was performed via a drop test. In brief, cultures of comparable density were serially diluted, spotted on plates and incubated at 25 °C for 5 days. Adult viability in *Drosophila* was calculated as the percentage of the number of adult flies with the appropriate genotype divided by the expected number for the cross. When indicated, a temperature of 29 °C was utilised to amplify GAL4 activity. For survival analysis, adult flies were maintained in vials at a density of 15 to 20 flies per vial. The percentage number of flies alive at each time point measured was determined by dividing the number of flies still alive by the initial number of flies in the vial and multiplying the value by 100. During their adult lifespan, flies were transferred to new vials routinely.

4.7. Puparial axial ratios

Puparial axial ratios were calculated by dividing the length by the width of the puparia, both of which were measured from still images.

4.8. Flight assay

In preparation for flight quantification, flies were first subjected to a 'warm-up' by inducing negative geotaxis in a new empty vial for 6 times. As described previously (Borg and Cauchi, 2013), the organisms were then introduced into the top of the Droso-Drome, which consisted of a 1 L glass bottle with a 9 cm diameter that was coated with an alcohol-based sticky fluid, and divided into 4 sectors, of 5 cm each, spanning a total height of 20 cm. The number of flies in each sector was counted, divided by the total number of flies assessed and multiplied by 100 to generate the percentage number of flies per sector. Flight ability is determined by the height or sector in which flies are distributed. To minimise variability and allow comparability, flight assays were performed by the same experimentalist. Flies with gross wing malformations evident after eclosion were excluded from the assay.

4.9. Drosophila activity monitoring assays

Automated monitoring of *Drosophila* activity was performed as described previously (Chiu et al., 2010). Flies selected for analysis were transferred to glass activity tubes containing apple juice with 2% agar at one end and a cotton plug at the other end. The tubes were then placed in a *Drosophila* activity monitor (TriKinetics Inc., Waltham, MA, USA) where their movements were recorded continuously at a culture temperature of 25 °C and a 12:12-h dark:light cycle. Five contiguous minutes of inactivity were taken as sleep/rest periods and were excluded when assessing the wake activity.

4.10. Fluorescence imaging and quantification

Yeast cells taken from plates were transferred into mounting medium with 5 μg/mL DAPI on a microscope slide and covered with a cover slip. Fluorescent images were captured using a Leica DMRA fluorescence microscope equipped with 100× Leica HCX PL APO 1.4-0.7 oil immersion objective and fitted with a Photometrics CoolSNAP HQ camera. DAPI-stained nuclei and GFP fluorescence were acquired via the blue DAPI channel (20 ms exposure) and the green GFP channel (500 ms exposure), respectively. Quantification of cell parameters was done via ImageJ (NIH). The line tool and the Analyze/Measure command was used to determine cell length after using the Analyze/Set Scale dialog to define spatial scale. Fluorescence signal was measured by first selecting the region of interest within the cell using the freehand selection tool followed by the Analyze/Measure command to determine area and integrated density. The corrected fluorescence signal was calculated as integrated density – (area of the selected region within cell x mean fluorescence of background readings) as previously described (Cappell et al., 2012).

4.11. Yeast two-hybrid analysis

Two-hybrid assays were performed with the CG1945 and Y187 strains (Clontech, Saint-Germain-en-Laye, France) (Vojtek et al., 1993). Baits and preys were obtained by PCR amplification of cDNA and ligation into the *pASΔΔ* and *pACT2st* vectors, respectively (Fromont-Racine et al., 2002). Primer sequences and PCR regimes are available upon request. cDNA clones for *Gemin3* (LD05563), *Smn* (LD23602), *Tgs1* (LD22407), *pICln* (SD10511) and *wmd* (HL01517) were obtained from the *Drosophila* Genomics Resource Centre (Indiana University, USA). The CG1945 strain was transformed with the pASΔΔ constructs and selected on –Trp plates while the Y187 strain was transformed with the pACT2st constructs and selected on –Leu plates. Bait and prey strains were mated overnight on rich YPD plates and diploids containing bait/prey combinations were selected on –Trp–Leu plates. Diploid yeast cells carrying bait/prey combinations were cultured in –Trp–Leu media and protein-protein interactions were screened by spotting serial dilutions on –Trp–Leu–His plates. Incubations were performed at 28 °C for 3 to 5 days. Quantification of yeast two-hybrid interactions was performed via the β-galactosidase assay. Cells were grown in –Trp–Leu selective medium to an $OD_{600} = 0.5$–1.0. Activity was measured from extracts as described previously (Guarente, 1983).

4.12. Statistical Analysis

Values are presented as means ± S.E.M. unless indicated otherwise. The unpaired *t*-test was used for all analyses to compare measures between 2 groups, namely, the mean values of the experimental genotype to the control genotype (GraphPad Prism v7.0a; GraphPad Software Inc., San Diego, CA, USA). For flight assays, comparative analysis was restricted to sector 1 of the Droso-Drome in view that this is the sector that mostly determines differences between fliers and non-fliers. Differences were deemed statistically significant if $p < 0.05$, and when this is the case, the exact *p*-value, the *t*-statistic (t) as well as the associated degrees-of-freedom (*df*) are presented.

Supplementary data to this article can be found online at http://dx.doi.org/10.1016/j.nbd.2016.06.015.

Acknowledgements

References

Barbarossa, A., et al., 2014. Characterization and in vivo functional analysis of the *Schizosaccharomyces pombe* ICLN gene. Mol. Cell. Biol. 34, 595–605.

Battle, D.J., et al., 2006. The Gemin5 protein of the SMN complex identifies snRNAs. Mol. Cell 23, 273–279.

Bellen, H.J., Yamamoto, S., 2015. Morgan's legacy: fruit flies and the functional annotation of conserved genes. Cell 163, 12–14.

Bischof, J., et al., 2013. A versatile platform for creating a comprehensive UAS-ORFeome library in Drosophila. Development 140, 2434–2442.

Boon, K.L., et al., 2015. Self-association of Trimethylguanosine Synthase Tgs1 is required for efficient snRNA/snoRNA trimethylation and pre-rRNA processing. Sci. Rep. 5, 11282.

Bordonne, R., 2000. Functional characterization of nuclear localization signals in yeast Sm proteins. Mol. Cell. Biol. 20, 7943–7954.

Borg, R., Cauchi, R.J., 2013. The gemin associates of survival motor neuron are required for motor function in Drosophila. PLoS One 8, e83878.

Borg, R., Cauchi, R.J., 2014. GEMINs: potential therapeutic targets for spinal muscular atrophy? Front. Neurosci. 8, 325.

Borg, R.M., et al., 2015. Genetic Interactions between the members of the SMN-gemins complex in Drosophila. PLoS One 10, e0130974.

Burghes, A.H., Beattie, C.E., 2009. Spinal muscular atrophy: why do low levels of survival motor neuron protein make motor neurons sick? Nat. Rev. Neurosci. 10, 597–609.

Campion, Y., et al., 2010. Specific splicing defects in S. pombe carrying a degron allele of the survival of motor neuron gene. EMBO J. 29, 1817–1829.

Cappell, K.M., et al., 2012. Multiple cancer testis antigens function to support tumor cell mitotic fidelity. Mol. Cell. Biol. 32, 4131–4140.

Carissimi, C., et al., 2005. Unrip is a component of SMN complexes active in snRNP assembly. FEBS Lett. 579, 2348–2354.

Cauchi, R.J., 2010. SMN and Gemins: 'we are family' ... or are we? Insights into the partnership between Gemins and the spinal muscular atrophy disease protein SMN. BioEssays 32, 1077–1089.

Cauchi, R.J., 2014. Gem depletion: amyotrophic lateral sclerosis and spinal muscular atrophy crossover. CNS Neurosci. Ther. 20, 574–581.

Cauchi, R.J., van den Heuvel, M., 2006. The fly as a model for neurodegenerative diseases: is it worth the jump? Neurodegener. Dis. 3, 338–356.

Cauchi, R.J., et al., 2008. A motor function for the DEAD-box RNA helicase, Gemin3, in Drosophila. PLoS Genet. 4, e1000265.

Cauchi, R.J., et al., 2010. Drosophila SMN complex proteins Gemin2, Gemin3, and Gemin5 are components of U bodies. Exp. Cell Res. 316, 2354–2364.

Chang, H.C., et al., 2008. Modeling spinal muscular atrophy in Drosophila. PLoS One 3, e3209.

Chari, A., et al., 2008. An assembly chaperone collaborates with the SMN complex to generate spliceosomal SnRNPs. Cell 135, 497–509.

Charroux, B., et al., 1999. Gemin3: a novel DEAD box protein that interacts with SMN, the spinal muscular atrophy gene product, and is a component of Gems. J. Cell Biol. 147, 1181–1193.

Chiu, J.C., et al., 2010. Assaying locomotor activity to study circadian rhythms and sleep parameters in Drosophila. J. Vis. Exp.

Craven, R.A., et al., 1998. Vectors for the expression of tagged proteins in Schizosaccharomyces pombe. Gene 221, 59–68.

Datta, P.K., et al., 1998. Identification of STRAP, a novel WD domain protein in transforming growth factor-beta signaling. J. Biol. Chem. 273, 34671–34674.

Dietzl, G., et al., 2007. A genome-wide transgenic RNAi library for conditional gene inactivation in Drosophila. Nature 448, 151–156.

Dworkin, I., Gibson, G., 2006. Epidermal growth factor receptor and transforming growth factor-beta signaling contributes to variation for wing shape in Drosophila melanogaster. Genetics 173, 1417–1431.

Fallini, C., et al., 2012. Spinal muscular atrophy: the role of SMN in axonal mRNA regulation. Brain Res. 1462, 81–92.

Fischer, U., et al., 2011. Biogenesis of spliceosomal small nuclear ribonucleoproteins. Wiley interdisciplinary reviews. RNA 2, 718–731.

Foust, K.D., et al., 2010. Rescue of the spinal muscular atrophy phenotype in a mouse model by early postnatal delivery of SMN. Nat. Biotechnol. 28, 271–274.

Fromont-Racine, M., et al., 2002. Building protein-protein networks by two-hybrid mating strategy. Methods Enzymol. 350, 513–524.

Gabanella, F., et al., 2005. The activity of the spinal muscular atrophy protein is regulated during development and cellular differentiation. Hum. Mol. Genet. 14, 3629–3642.

Gabanella, F., et al., 2007. Ribonucleoprotein assembly defects correlate with spinal muscular atrophy severity and preferentially affect a subset of spliceosomal snRNPs. PLoS One 2, e921.

Gerbino, V., et al., 2013. Mislocalised FUS mutants stall spliceosomal snRNPs in the cytoplasm. Neurobiol. Dis. 55, 120–128.

Grice, S.J., Liu, J.L., 2011. Survival motor neuron protein regulates stem cell division, proliferation, and differentiation in Drosophila. PLoS Genet. 7, e1002030.

Grimm, C., et al., 2013. Structural basis of assembly chaperone-mediated snRNP formation. Mol. Cell 49, 692–703.

Grimmler, M., et al., 2005. Unrip, a factor implicated in cap-independent translation, associates with the cytosolic SMN complex and influences its intracellular localization. Hum. Mol. Genet. 14, 3099–3111.

Guarente, L., 1983. Yeast promoters and lacZ fusions designed to study expression of cloned genes in yeast. Methods Enzymol. 101, 181–191.

Guruharsha, K.G., et al., 2011. A protein complex network of Drosophila melanogaster. Cell 147, 690–703.

Imlach, W.L., et al., 2012. SMN is required for sensory-motor circuit function in Drosophila. Cell 151, 427–439.

Jia, Y., et al., 2012. Early embryonic lethality of mice with disrupted transcription cofactor PIMT/NCOA6IP/Tgs1 gene. Mech. Dev. 129, 193–207.

Kariya, S., et al., 2014. Requirement of enhanced Survival Motoneuron protein imposed during neuromuscular junction maturation. J. Clin. Invest. 124, 785–800.

Komonyi, O., et al., 2005. DTL, the Drosophila homolog of PIMT/Tgs1 nuclear receptor co-activator-interacting protein/RNA methyltransferase, has an essential role in development. J. Biol. Chem. 280, 12397–12404.

Kroiss, M., et al., 2008. Evolution of an RNP assembly system: a minimal SMN complex facilitates formation of UsnRNPs in Drosophila melanogaster. Proc. Natl. Acad. Sci. U. S. A. 105, 10045–10050.

Lau, C.K., et al., 2009. Gemin5-snRNA interaction reveals an RNA binding function for WD repeat domains. Nat. Struct. Mol. Biol. 16, 486–491.

Le, T.T., et al., 2011. Temporal requirement for high SMN expression in SMA mice. Hum. Mol. Genet. 20, 3578–3591.

Lemm, I., et al., 2006. Ongoing U snRNP biogenesis is required for the integrity of Cajal bodies. Mol. Biol. Cell 17, 3221–3231.

Li, D.K., et al., 2014. SMN control of RNP assembly: from post-transcriptional gene regulation to motor neuron disease. Semin. Cell Dev. Biol. 32C, 22–29.

Lotti, F., et al., 2012. An SMN-dependent U12 splicing event essential for motor circuit function. Cell 151, 440–454.

Lutz, C.M., et al., 2011. Postsymptomatic restoration of SMN rescues the disease phenotype in a mouse model of severe spinal muscular atrophy. J. Clin. Invest. 121, 3029–3041.

Ma, Y., et al., 2005. The Gemin6–Gemin7 heterodimer from the survival of motor neurons complex has an Sm protein-like structure. Structure 13, 883–892.

Maundrell, K., 1993. Thiamine-repressible expression vectors pREP and pRIP for fission yeast. Gene 123, 127–130.

Monani, U.R., De Vivo, D.C., 2014. Neurodegeneration in spinal muscular atrophy: from disease phenotype and animal models to therapeutic strategies and beyond. Future Neurol. 9, 49–65.

Moreno, S., et al., 1991. Molecular genetic analysis of fission yeast Schizosaccharomyces pombe. Methods Enzymol. 194, 795–823.

Mouaikel, J., et al., 2002. Hypermethylation of the cap structure of both yeast snRNAs and snoRNAs requires a conserved methyltransferase that is localized to the nucleolus. Mol. Cell 9, 891–901.

Mouaikel, J., et al., 2003. Interaction between the small-nuclear-RNA cap hypermethylase and the spinal muscular atrophy protein, survival of motor neuron. EMBO Rep. 4, 616–622.

Ogawa, C., et al., 2009. Role of survival motor neuron complex components in small nuclear ribonucleoprotein assembly. J. Biol. Chem. 284, 14609–14617.

Otter, S., et al., 2007. A comprehensive interaction map of the human survival of motor neuron (SMN) complex. J. Biol. Chem. 282, 5825–5833.

Pellizzoni, L., et al., 1998. A novel function for SMN, the Spinal Muscular Atrophy disease gene product, in pre-mRNA splicing. Cell 95, 615–624.

Pu, W.T., et al., 1999. pICln inhibits snRNP biogenesis by binding core spliceosomal proteins. Mol. Cell. Biol. 19, 4113–4120.

Pu, W.T., et al., 2000. ICln is essential for cellular and early embryonic viability. J. Biol. Chem. 275, 12363–12366.

Rajendra, T.K., et al., 2007. A Drosophila melanogaster model of spinal muscular atrophy reveals a function for SMN in striated muscle. J. Cell Biol. 176, 831–841.

Reiner, J.E., Datta, P.K., 2011. TGF-beta-dependent and -independent roles of STRAP in cancer. Front. Biosci. 16, 105–115.

Sen, A., et al., 2013. Genetic circuitry of Survival motor neuron, the gene underlying spinal muscular atrophy. Proc. Natl. Acad. Sci. U. S. A. 110, E2371–E2380.

Shpargel, K.B., et al., 2009. Gemin3 is an essential gene required for larval motor function and pupation in Drosophila. Mol. Biol. Cell 20, 90–101.

Simossis, V.A., Heringa, J., 2005. PRALINE: a multiple sequence alignment toolbox that integrates homology-extended and secondary structure information. Nucleic Acids Res. 33, W289–W294.

So, B.R., et al., 2016. A U1 snRNP-specific assembly pathway reveals the SMN complex as a versatile hub for RNP exchange. Nat. Struct. Mol. Biol. 23, 225–230.

Timmerman, C., Sanyal, S., 2012. Behavioral and electrophysiological outcomes of tissue-specific Smn knockdown in Drosophila melanogaster. Brain Res. 1489, 66–80.

Vojtek, A.B., et al., 1993. Mammalian Ras interacts directly with the serine/threonine kinase Raf. Cell 74, 205–214.

Wan, L., et al., 2005. The survival of motor neurons protein determines the capacity for snRNP assembly: biochemical deficiency in spinal muscular atrophy. Mol. Cell. Biol. 25, 5543–5551.

Winkler, C., et al., 2005. Reduced U snRNP assembly causes motor axon degeneration in an animal model for spinal muscular atrophy. Genes Dev. 19, 2320–2330.

Workman, E., et al., 2009. A SMN missense mutation complements SMN2 restoring snRNPs and rescuing SMA mice. Hum. Mol. Genet. 18, 2215–2229.

Workman, E., et al., 2012. Spliceosomal small nuclear ribonucleoprotein biogenesis defects and motor neuron selectivity in spinal muscular atrophy. Brain Res. 1462, 93–99.

Yan, X., et al., 2003. A novel domain within the DEAD-box protein DP103 is essential for transcriptional repression and helicase activity. Mol. Cell. Biol. 23, 414–423.

Yong, J., et al., 2010. Gemin5 delivers snRNA precursors to the SMN complex for snRNP biogenesis. Mol. Cell 38, 551–562.

Yu, Y., et al., 2015. U1 snRNP is mislocalized in ALS patient fibroblasts bearing NLS mutations in FUS and is required for motor neuron outgrowth in zebrafish. Nucleic Acids Res. 43, 3208–3218.

Zhang, R., et al., 2011. Structure of a key intermediate of the SMN complex reveals Gemin2's crucial function in snRNP assembly. Cell 146, 384–395.

Zhang, Z., et al., 2013. Dysregulation of synaptogenesis genes antecedes motor neuron pathology in spinal muscular atrophy. Proc. Natl. Acad. Sci. U. S. A. 110, 19348–19353.